Delineation of Intake Protection Zones in the CRCA jurisdiction – Modeling Approach

April 27, 2009

Prepared by:

Shastri Paturi and Leon Boegman

Centre for Water and the Environment

Department of Civil Engineering

Queen's University

Kingston, ON

Canada K7L 3N6

Prepared for:

Cataraqui Region Conservation Authority

Glenburnie, ON

Canada K0H 1S0

Table of Contents

List of Figures

List of Tables

1. Introduction

Under an agreement with the Province of Ontario (Ministry of Environment), the Cataraqui Region Conservation Authority (CRCA) is coordinating a source water protection plan for the watersheds in its jurisdiction. These watersheds include the Napanee to Brockville corridor of eastern Lake Ontario and the upper St. Lawrence River, where there are eight municipal drinking water intakes (figure 1), and treating water for approximately 170,000 residents based on 2004 Environment Canada numbers (about 9500 of those are outside the CRCA in Napanee) .To protect these drinking water intakes from contamination and quantify the transport pathways of contaminants from known and possible sources, a hydrodynamic technical study is being undertaken to determine the flow characteristics in the region. The study conducted under collaboration between the CRCA, the National Water Research Institute of Environment Canada and the Centre for Water and Environment at Queen's University, combines field observation and computer modeling to determine the flow characteristics in the region.

The hydrodynamic model flows are analyzed to determine Intake Protection Zones (IPZ) surrounding each of the eight municipal surface water intakes. The purpose of these zones is to determine threats in land and water usage around surface water intakes that could lead to vulnerabilities in the water supply.

The results from the numerical model are validated against the field observations to ensure confidence in the simulated flow field and IPZ delineations.

2. IPZ delineation

For Eastern Lake Ontario and the upper St. Lawrence River, three IPZs have been delineated (Ontario Ministry of the Environment, 2005 a,b.).

- IPZ-1: The Great Lakes IPZ-1 is a radius of 1 km set around the intake. The Great Lakes Connecting Channel IPZ-1 delineation consists of a semi-circle of 1 km radius upstream, with a rectangle 2-km wide measuring a distance of 100 m downstream. The downstream distance compensates for possible localized flow reversals in the channels from the influences of wind and/or channel operations for hydroelectric or navigation purposes.

- IPZ-2: The IPZ-2 is the distance associated with a two-hour time of travel of a fluid parcel to the intake under 10-yr storm conditions. The two-hour travel time has been requested by plant operators to provide sufficient time for reporting and plant closure in the event of a contaminant spill.

- IPZ-3: The IPZ-3 was initially considered to be the distance associated with a two-hour time of travel of a fluid parcel to the intake under 100-year storm conditions (Ontario

Ministry of the Environment, 2005a,b). Since the completion of the results presented herein, the IPZ-3 delineation has been changed to encompass any contaminants released during an extreme event that may be transported to the intake. In this report, the IPZ-3 will be presented according to the original definitions and new IPZ-3 will be delineated in a later study.

3. Model

Simulations were conducted using the three-dimensional (3D), z-coordinate, hydrodynamic Estuary and Lake Computer Ocean Model (ELCOM) described by Hodges (2000) and Hodges et al. (2000). ELCOM solves for the Reynolds-averaged, hydrostatic, Boussinesq, Navier-Stokes, and scalar transport equations. ELCOM has an eddy-viscosity/diffusivity closure scheme for horizontal turbulence correlations and employs the ULTIMATE QUICKEST advection scheme for scalars. Vertical mixing is computed using an explicit turbulent kinetic energy budget closure scheme that is applied to each individual water column of the 3D flow matrix during each model time step (Hodges et al. 2000). Turbulent kinetic energy is introduced at the surface from surface wind stress and at the lake bed through a bottom shear drag coefficient parameterization. The extent of mixing performed in a single model time step is limited by a mixing time scale, allowing for partial mixing of vertically adjacent cells (Laval et al. 2003b). Momentum is introduced into the water column by wind stress at the surface and is distributed vertically by the mixed-layer model.

A uniform horizontal grid resolution was applied with a 300 m x 300 m resolution. The vertical grid has 69 layers with varying resolution. For the top 16 m (the maximum depth of field observations), the vertical resolution is maintained at 0.5 m with decreasing resolution in the layers from 16 m to 70 m(varying from 1m to 2.6m). The model grid covers the region from the Sandhurst Shores intake in the south-west to the Brockville intake in the north-east (figure 1).

3.1. Bathymetry

The bathymetric grid (figure 2) was generated using datasets from two sources. Bathymetric soundings (331,706 in total) are interpolated for the region between Kingston and Cornwall (source: Aaron Thompson, Environment Canada). Gridded bathymetric data with 3 second resolution are used for the region between Kingston and Prince Edward County. The gridded data were obtained from the National Geophysical Data Centre (http://www.ngdc.noaa.gov/mgg/gdas/gd_designagrid.html). The horizontal datum is in UTM coordinates, Zone 17, NAD83, metres. The vertical datum is IGLD 85 in metres. The maximum depth in the model is 70 m.

3.2. Initial and boundary conditions

The simulation period was 190 days from 13 April, 2006 to 19 October, 2006 with a time step of 5 minutes. Simulations were cold started (i.e., the fluid was at rest). An observed vertical temperature was used as an initial condition from a thermister mooring at station 1263 (figure 3) in the Kingston basin.

The bottom boundary was modeled in ELCOM as a turbulent boundary layer, with free slip side boundaries. Stress at the free surface due to wind is modeled as a momentum source applied to the surface wind-mixed layer (Hodges et al., 2000). Wind stress is calculated from wind velocity using a bulk formulation

$$\tau_w = \rho_a C_D |u_w| u_w \qquad (1)$$

Where ρ_a is the density of air, taken as 1.2 kg m^{-3}, C_D is a coefficient of drag taken as 0.0005 and u_w is the wind velocity adjusted to ten meters above the water surface.

The surface boundary conditions were specified with measured meteorological parameters from Station 1263 in the Kingston basin (source: Ram Yerubandi, Environment Canada). The open boundaries were forced with observed water levels from Kingston (south-west boundary) and Brockville (north-east boundary) stations (http://www.meds-sdmm.dfo-mpo.gc.ca/meds/databases/TWL/TWL_station_list_e.asp?user=MEDS&region=CA&tst=1) and the temperature data as scalars from thermistor chain deployed at station 1263. Outflow volume (m^3 s^{-1}) from the St. Lawrence River measured at Cornwall was specified the north-east boundary to account for the flow through the St. Lawrence River (source: Len Falkiner, Great Lakes St. Lawrence Regulation Office, Environment Canada).

4. Observational Data

Field observations of water column temperature and current speed and direction were collected at stations 1262, 1263, 1264, 1265 during 2006 and 2007 by NWRI Environment Canada (figure 3). Meteorological data was also collected at station 1263 (figure 4).

4.1. Reconstruction of 10-year and 100-year wind events

To delineate the IPZ-2 and IPZ-3, the model was run for the 2006 season with surface winds that were scaled such the maximum gust matched 10-yr storm conditions (23.3 ms^{-1}) and 100-yr storm conditions (28.6 ms^{-1}), as observed at the Kingston Airport located nearby on the shore of Lake Ontario (National Building Code of Canada 2005). To account for seasonal differences in

wind direction, lake level and stratification, we scaled the maximum gust observed during the spring (21.5 ms^{-1} on day 168), summer (24.0 ms^{-1} on day 192) and fall (15.6 ms^{-1} on day 286) seasons.

The 10-yr and 100-yr 1-hr average wind gusts at Kingston Airport (figure 5) were measured at 10 m above the surface, and so were scaled from 10 m to the 3.3 m height of the St. 1263 wind anemometer using a power law relation (Schertzer 1987), giving 19.89 ms^{-1} and 24.38 ms^{-1}, respectively. The winds were then adjusted over 24-hr storm duration (maximum gust plus/minus 12 hrs) such that the maximum 1-hr average wind gust matched the 10-yr or 100-yr condition corrected to 3.3 m. This procedure was repeated for the spring, summer and fall storm events.

5. Model Runs

The model was run for three cases. In case 1, the model was forced with measured wind speeds (as described in section 3.1). For cases 2 and 3, the model was forced with the reconstructed 10-yr and 100-yr winds, respectively. All other boundary and initial conditions remained the same in each case. To enable model validation, water level, temperature and currents were output at the locations of the field observations. To enable IPZ delineation, temperature and currents were also output at the locations of the drinking water intakes. Extensive model calibration was not required because ELCOM has been shown to capture the dynamics of lakes, rivers and coastal oceans of varying size (1km < diameter < 100 km) using a relatively standard set of parameters.

6. Results

Simulated water level, temperature and currents were compared with observations from stations 1262, 1263 and 1264 for case 1 to assess the model performance. The modelled currents from case 2 and 3 (10-yr storm and 100-yr storm events) were post-processed in MATLAB to generate 2-hr reverse progressive vector diagrams whose extent delineates the appropriate IPZs.

6.1. Comparison with field observations

The modelled water level comparison for Kingston and Brockville (figure 6) shows that the model has been able to capture the hydraulic flow without including flows from tributaries entering into the St. Lawrence River. Tributary flows into the St. Larwrence River account for less that 2% of the total river flow (Tsanis et al., 1991).

Figures 7-10 show comparisons of model temperature with observed temperature for Stn(s) 1262, 1263, 1264 and 1265 respectively. Stn 1263 (figure 8) and 1265 (figure 10) show a sharp thermocline at depth 15m. The modeled thermocline is not as abrupt as observed due to

numerical diffusion (Laval et al. 2002) and discrete nature of the horizontal and vertical grid resolution. The warming of the water column and temporal evolution of the stratification are well simulated during the summer months (days 180-280). The erosion of stratification and fall cooling are also well modeled.

At all stations, the maximum modelled temperature is ~ 2^{o}C colder than the maximum observed temperature. This result is consistent with application of ELCOM to other Laurentian Lakes (e.g., Rao et al. 2009) and may be due to the need to adjust the long and short wave radiation by ~15% (Laval et al. 2003) to correctly model surface temperatures.

Comparison of the modeled east-west current profiles at Stn 1263 (figure 11) reveals that directions are well modeled, but the model occasionally overestimates the depth to which the strong surface currents penetrate (e.g., day 135 and day 190). Comparison of the observed and modelled north-south current profiles at Stn 1263 (figure 12) shows again that the current directions are well modeled, but here the model occasionally underestimates the depth to which the strong surface currents penetrate (e.g., day 160 and 190). These differences may be due to the topographic differences between the 300 m bathymetric grid and actual bathymetry (Hall 2008) or spatial variability in the surface wind field (Laval et al., 2003), which is not modeled.

At Stn 1264, the model underestimates the north-south current magnitude by 5-10cms^{-1} in the surface layer (figure 13). The simulated east-west component (figure 14) is underestimated in magnitude by 10-15cms^{-1} during the fall with strong current magnitudes in the bottom layers (10-15m) as compared to observed velocities. This is a region of seasonal wind-induced flow reversal in the St. Lawrence River and this process is not well captured, potentially due to the limitations in the vertical grid resolution.

The current meter comparison at Stn 1265 (figure 15) reveals that the modeled 10 m currents are much stronger than observed due to the interaction of the surface wind-driven lacustrine flow and the bottom riverine hydraulic flow. Overall the current direction is consistent with the field observations.

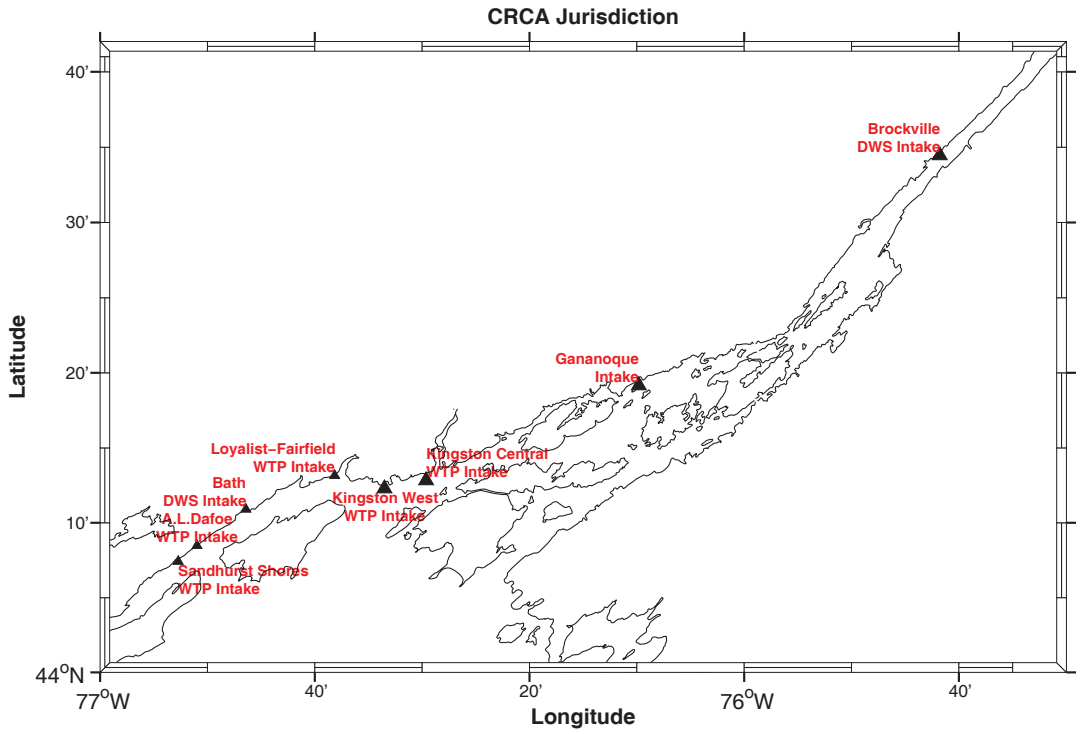

Figure 1. Cataraqui Region Conservation Authority drinking water intake locations.

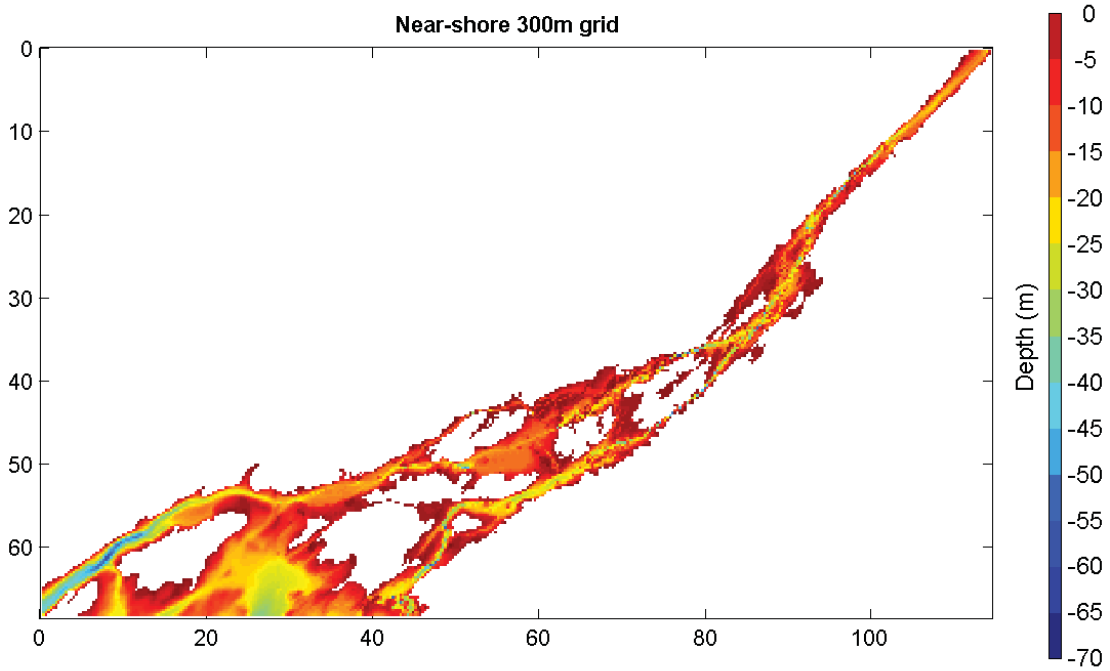

Figure 2. Bathymetry map of the near-shore model on a 300m uniform horizontal grid.

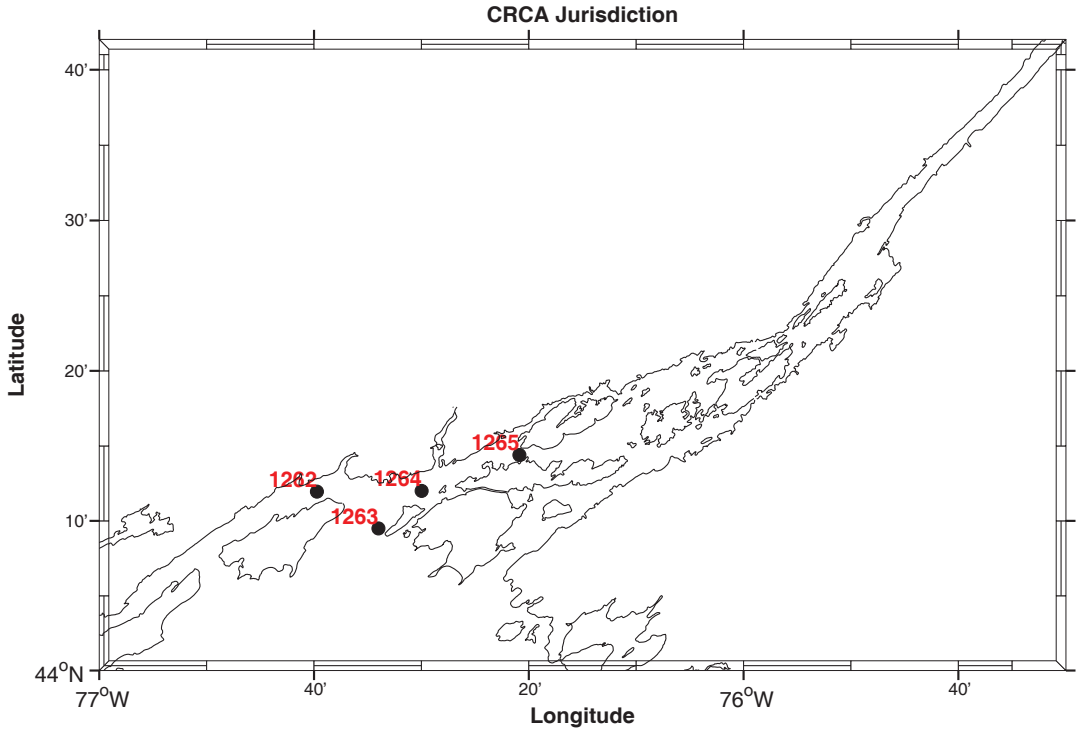

Figure 3. Map showing locations of observation stations 1262, 1263, 1264, 1265 used for comparison with model results.

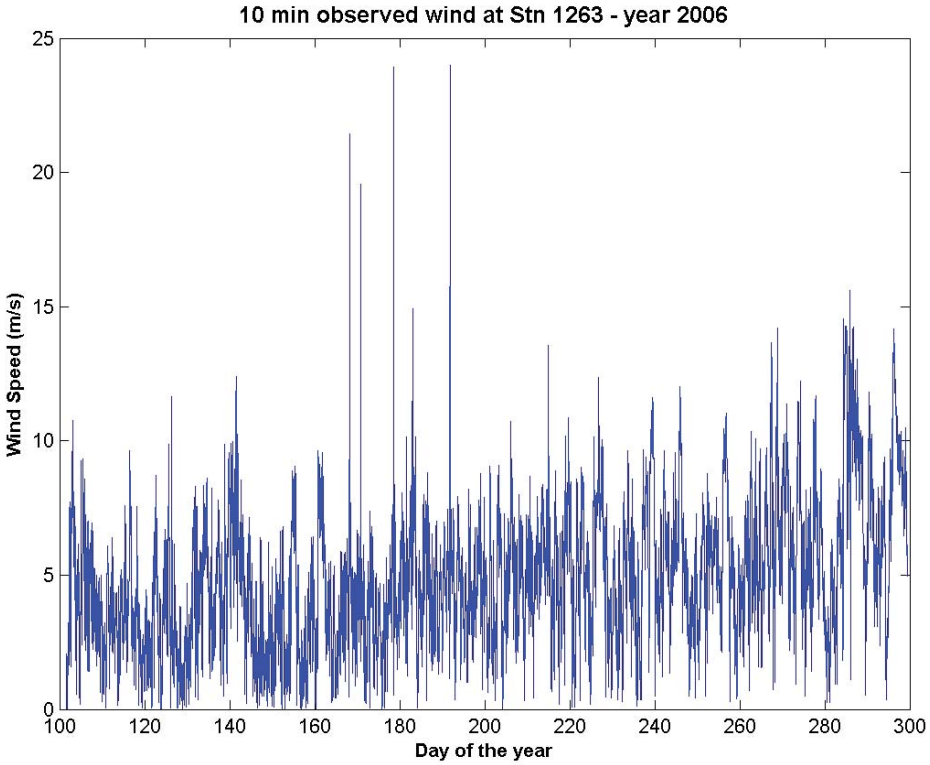

Figure 4. Wind data collected at Stn 1263 during 2006. Wind data is collected at 3m above the surface.

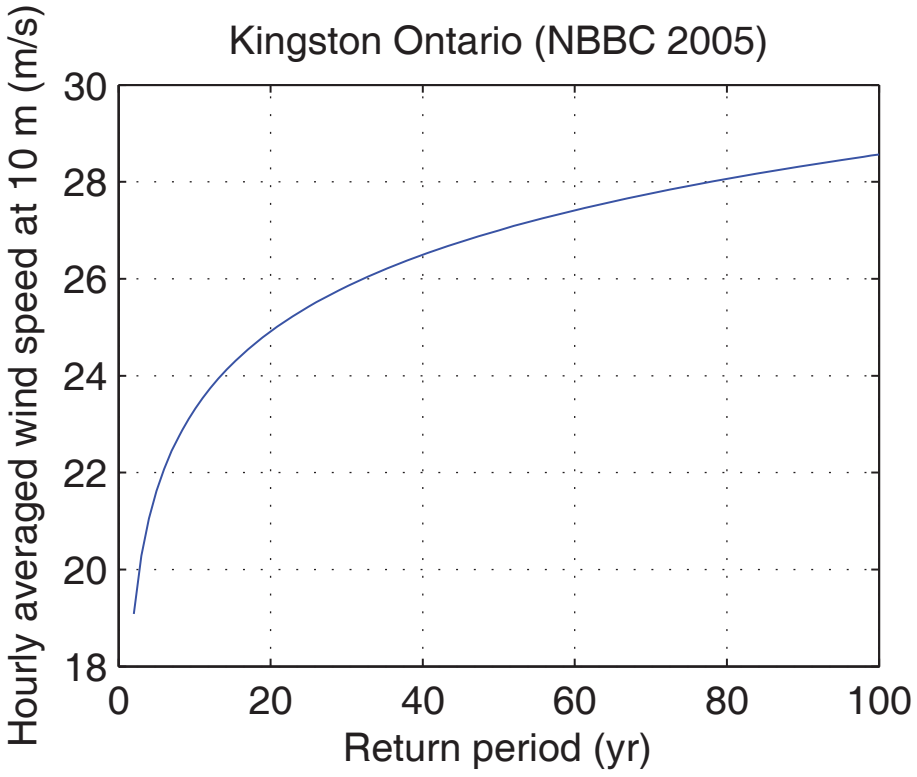

Figure 5. Return period of wind gusts measured at Kingston Airport. Wind data is 1 hr averages measured at 10-m above the land surface. From the National Building Code of Canada (2005).

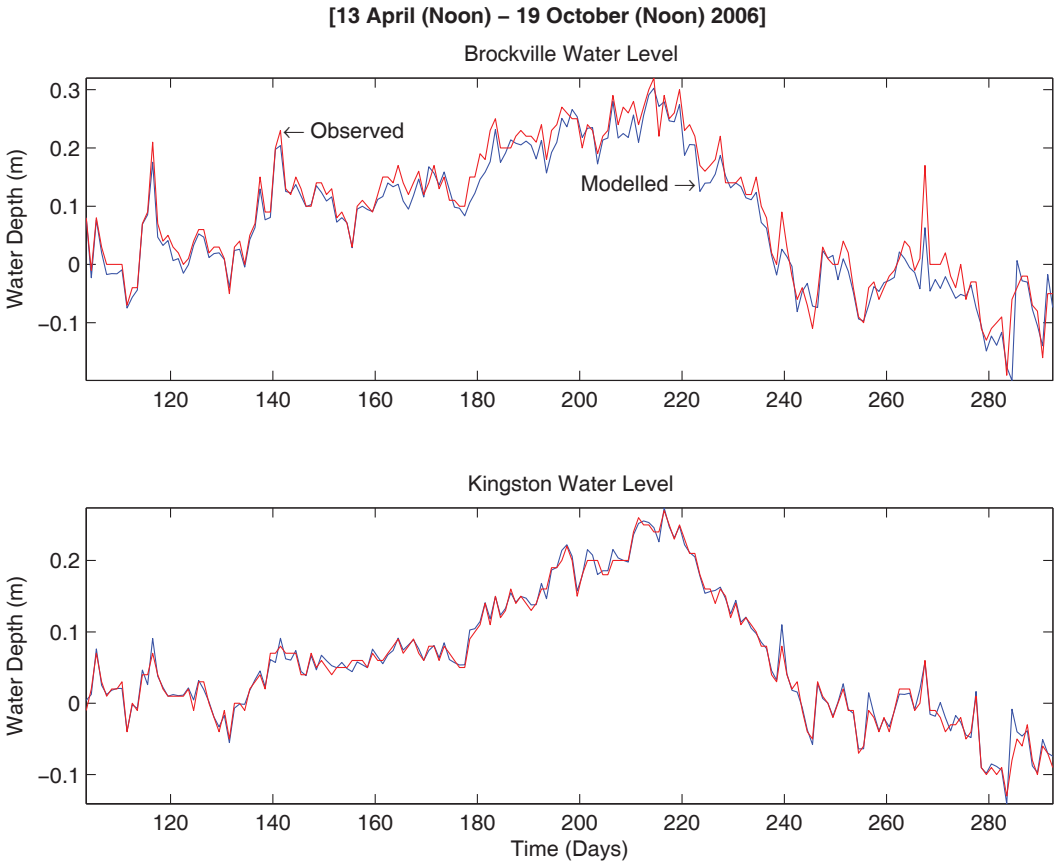

Figure 6. Observed and simulated water level comparison at Brockville and Kingston.

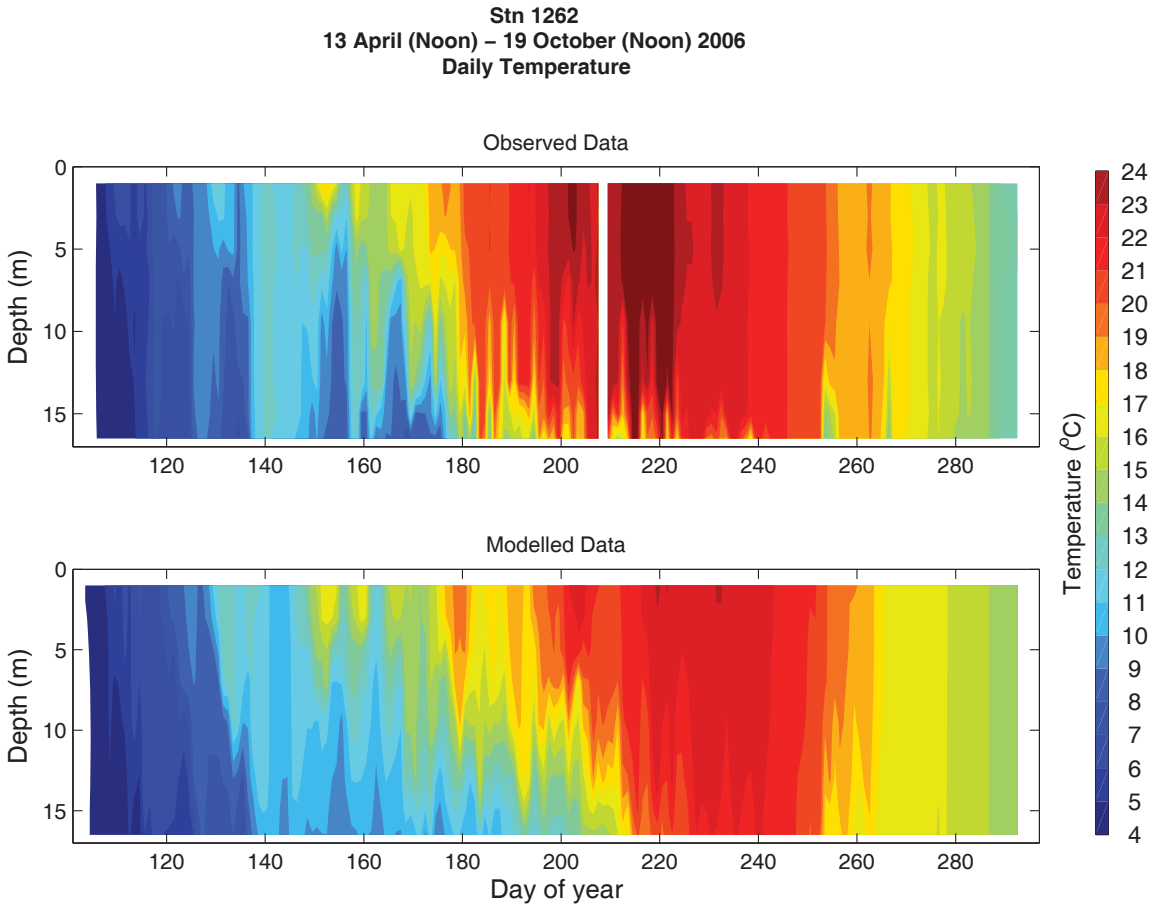

Figure 7. Daily observed and simulated temperature profile comparison at Stn 1262. Observed data (10 min) were collected by Environment Canada using Onset Tidbit temperature loggers located at depth of 1, 3, 5, 7, 9.5, 13, 15 and 16.5 m. Modelled temperature data was interpolated at the observed depths.

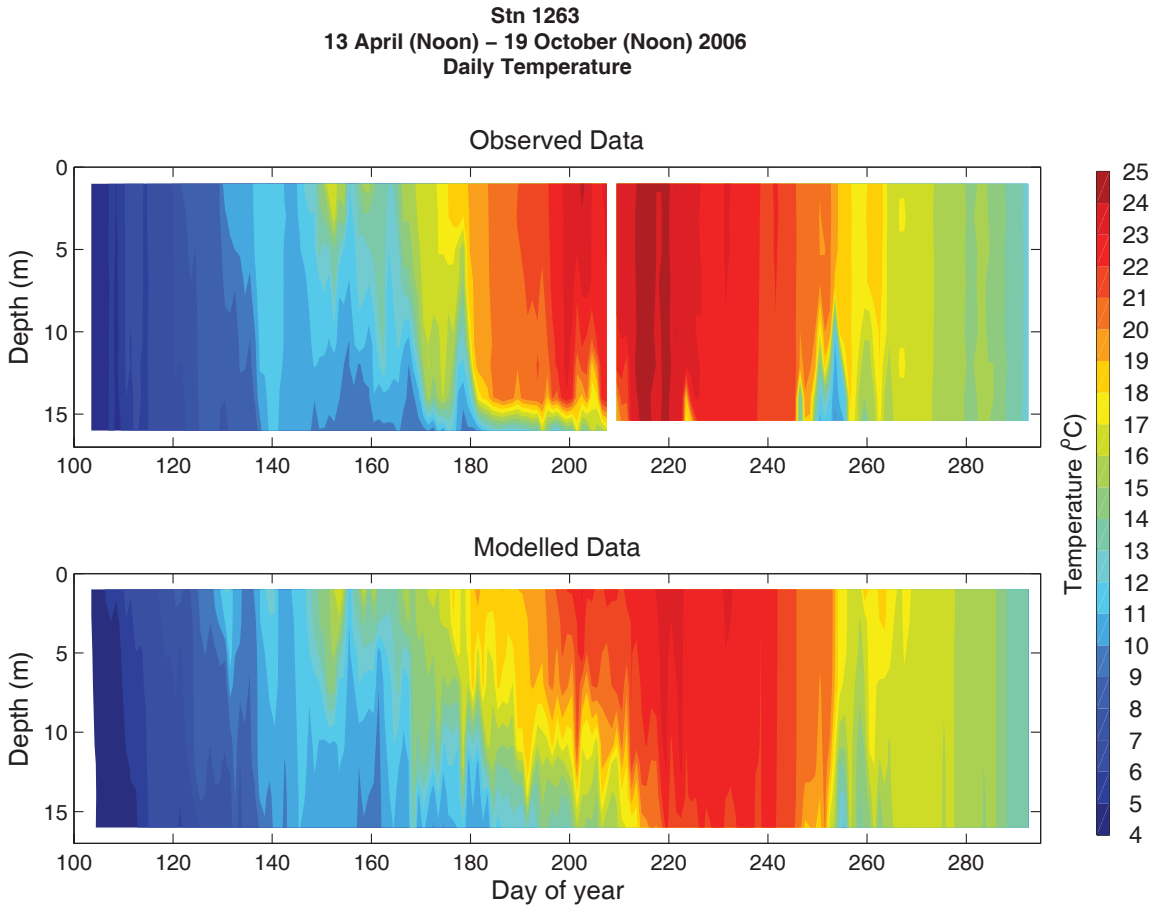

Figure 8. Daily observed and simulated temperature profile comparison at Stn 1263. Observed data (10 min) were collected by Environment Canada using Onset Tidbit temperature loggers located at depth of 1, 3, 5, 7, 10.8, 12, 14 and 16 m. Modelled temperature data was interpolated at the observed depths.

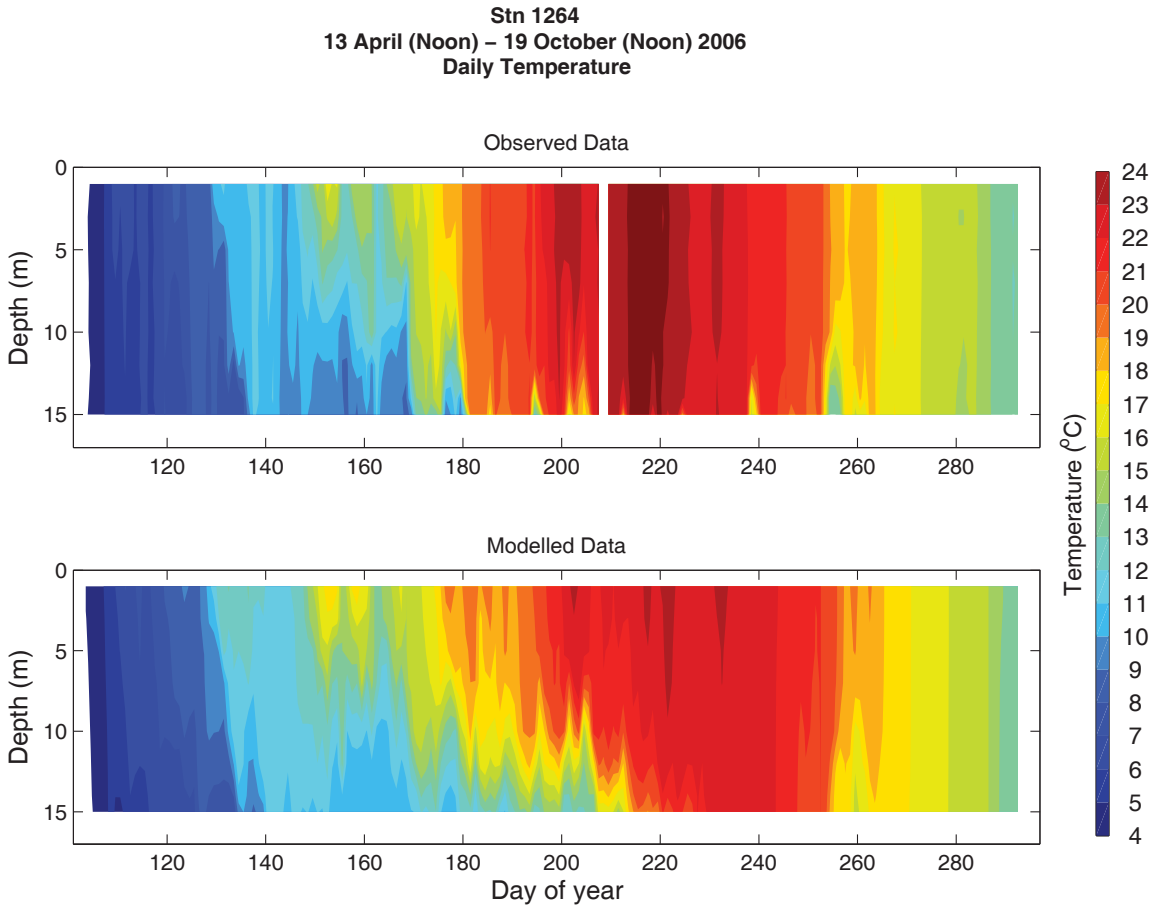

Figure 9. Daily observed and simulated temperature profile comparison at Stn 1264. Observed data (10 min) were collected by Environment Canada using Onset Tidbit temperature loggers located at depth of 1, 3, 5, 7, 10, 12, 14 and 15 m. Modelled temperature data was interpolated at the observed depths.

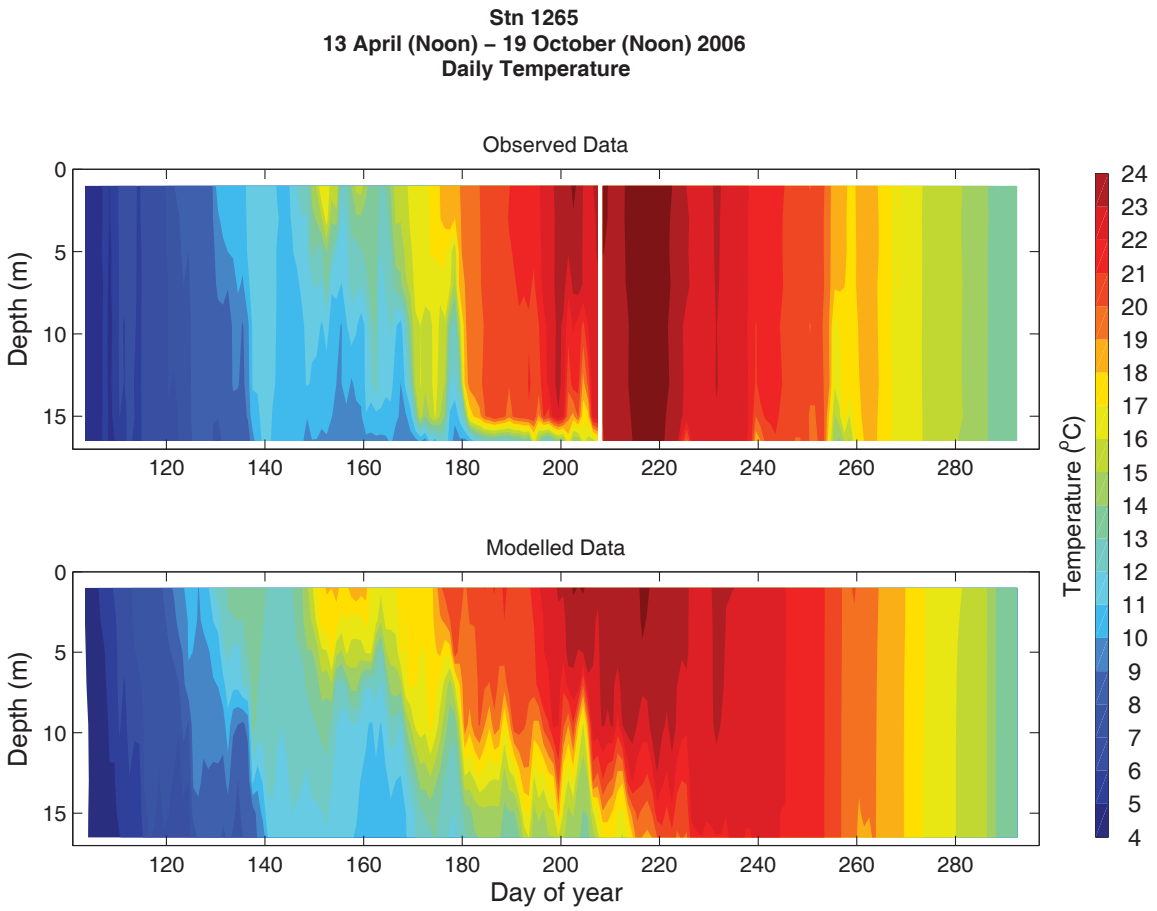

Figure 10. Daily observed and simulated temperature profile comparison at Stn 1265. Observed data (10 min) were collected by Environment Canada using Onset Tidbit temperature loggers located at depth of 1, 3, 5, 7, 9.5, 13, 15 and 16.5 m. Modelled temperature data was interpolated at the observed depths.

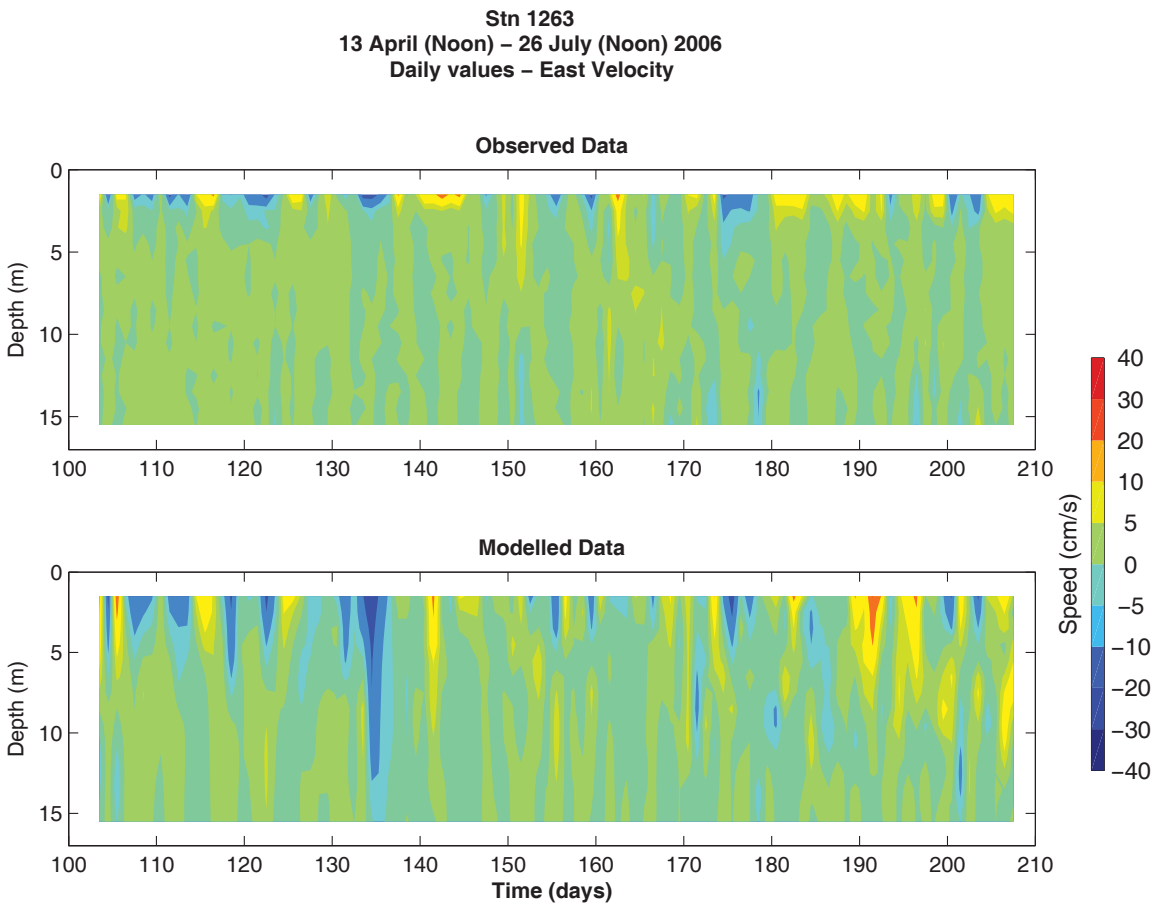

Figure 11. Daily observed and simulated East Velocity (U-component) comparison at Stn 1263. Observed data were collected by Environment Canada using an RDI Workhouse acoustic Doppler current profiler with 1 m vertical bins and a 30 min sampling frequency.

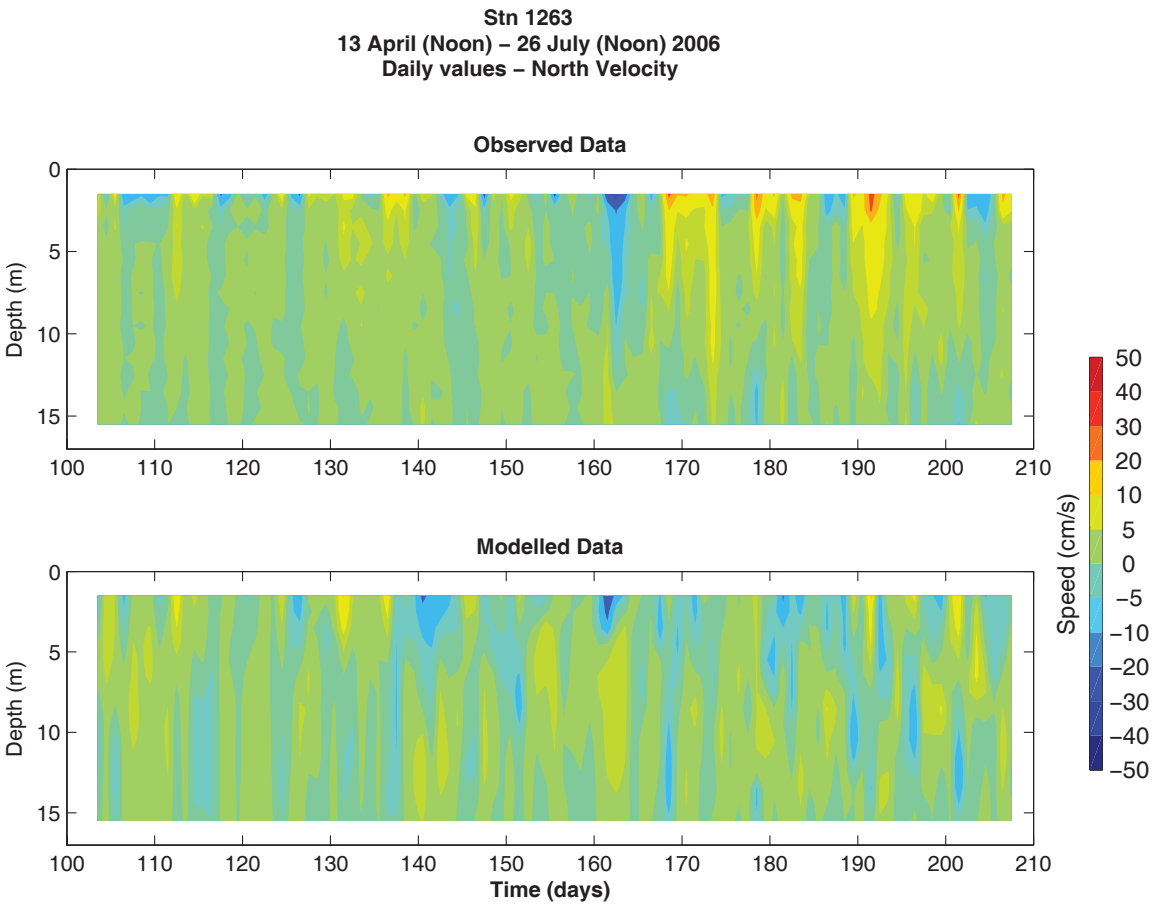

Figure 12. Daily observed and simulated North Velocity (V-component) comparison at Stn 1263. Observed data were collected by Environment Canada using an RDI Workhouse acoustic Doppler current profiler with 1 m vertical bins and a 30 min sampling frequency.

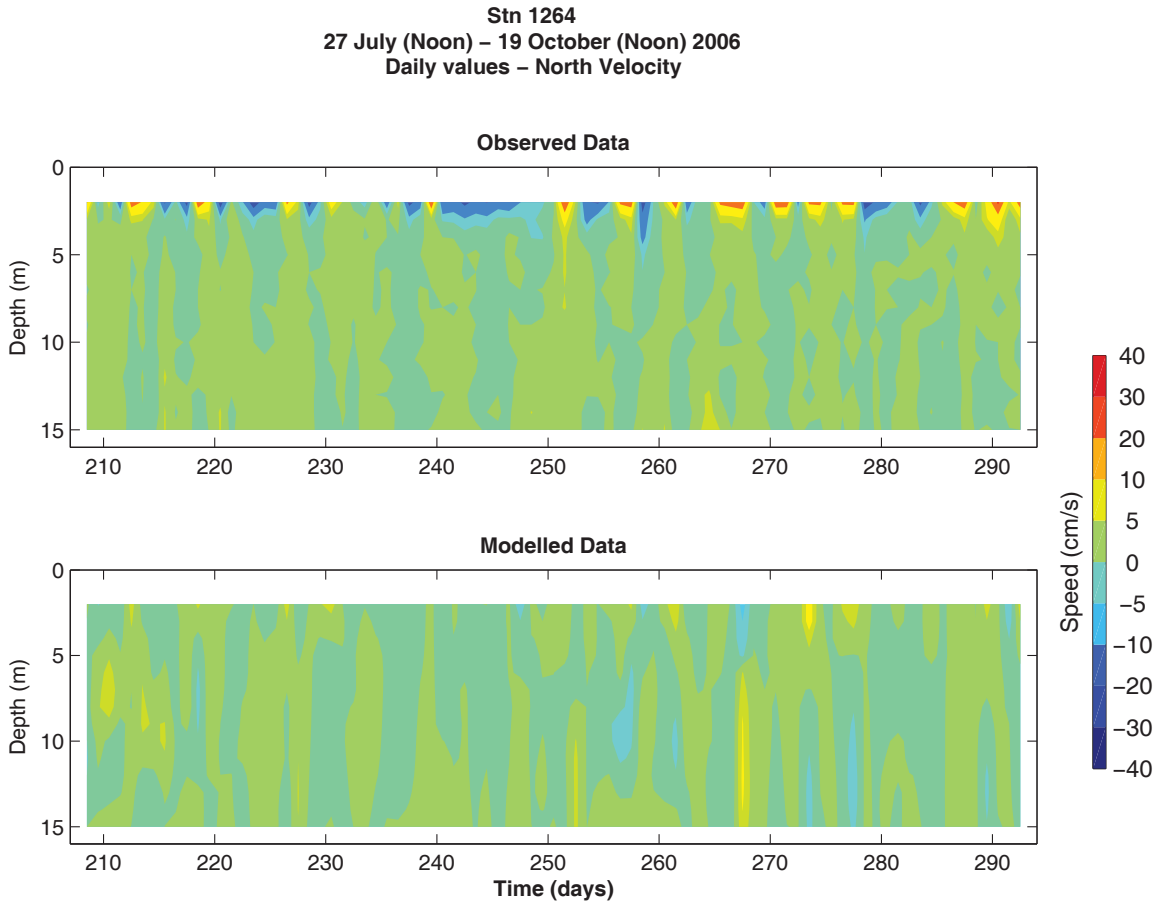

Figure 13. Daily observed and simulated North Velocity (V-component) comparison at Stn 1264. Observed data were collected by Environment Canada using an RDI Workhouse acoustic Doppler current profiler with 1 m vertical bins and a 30 min sampling frequency.

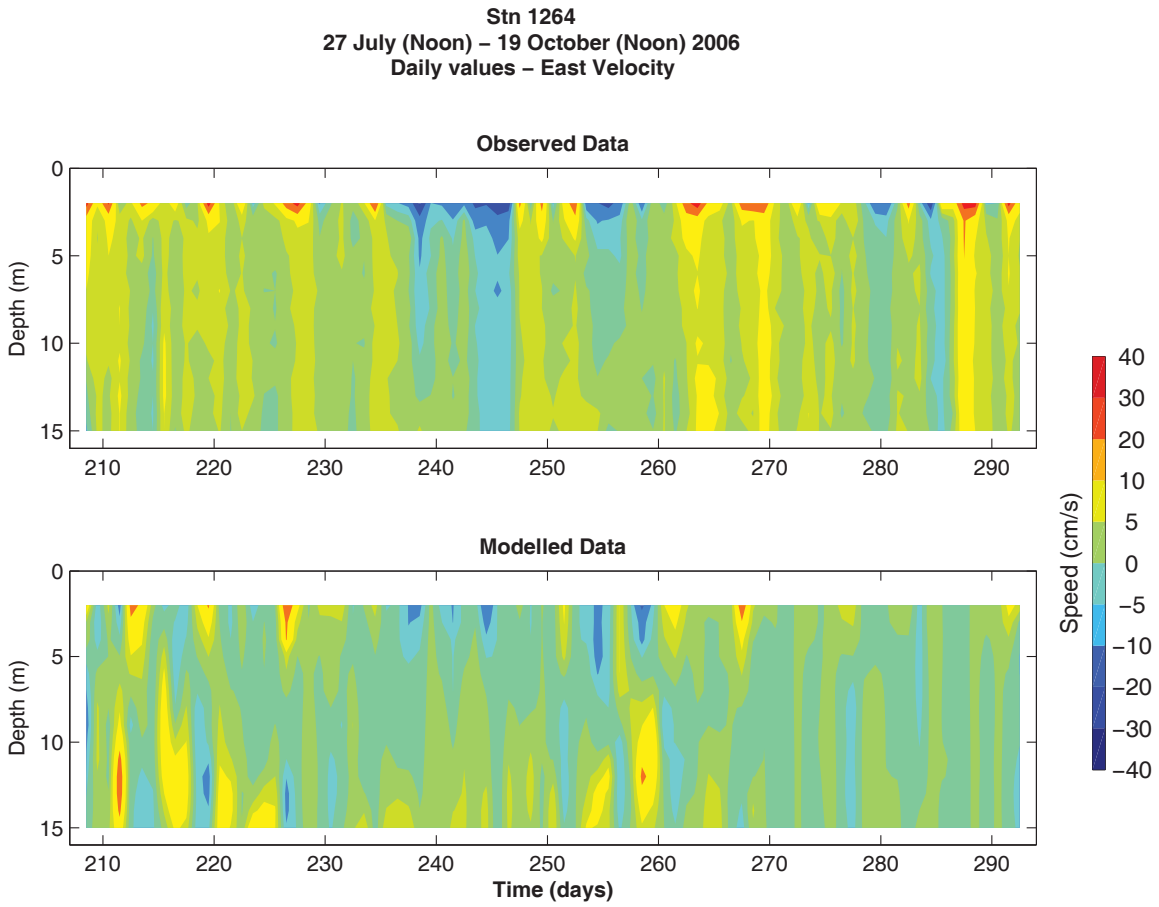

Figure 14. Observed and simulated East Velocity (U-component) comparison at Stn 1264. Observed data were collected by Environment Canada using an RDI Workhouse acoustic Doppler current profiler with 1 m vertical bins and a 30 min sampling frequency.

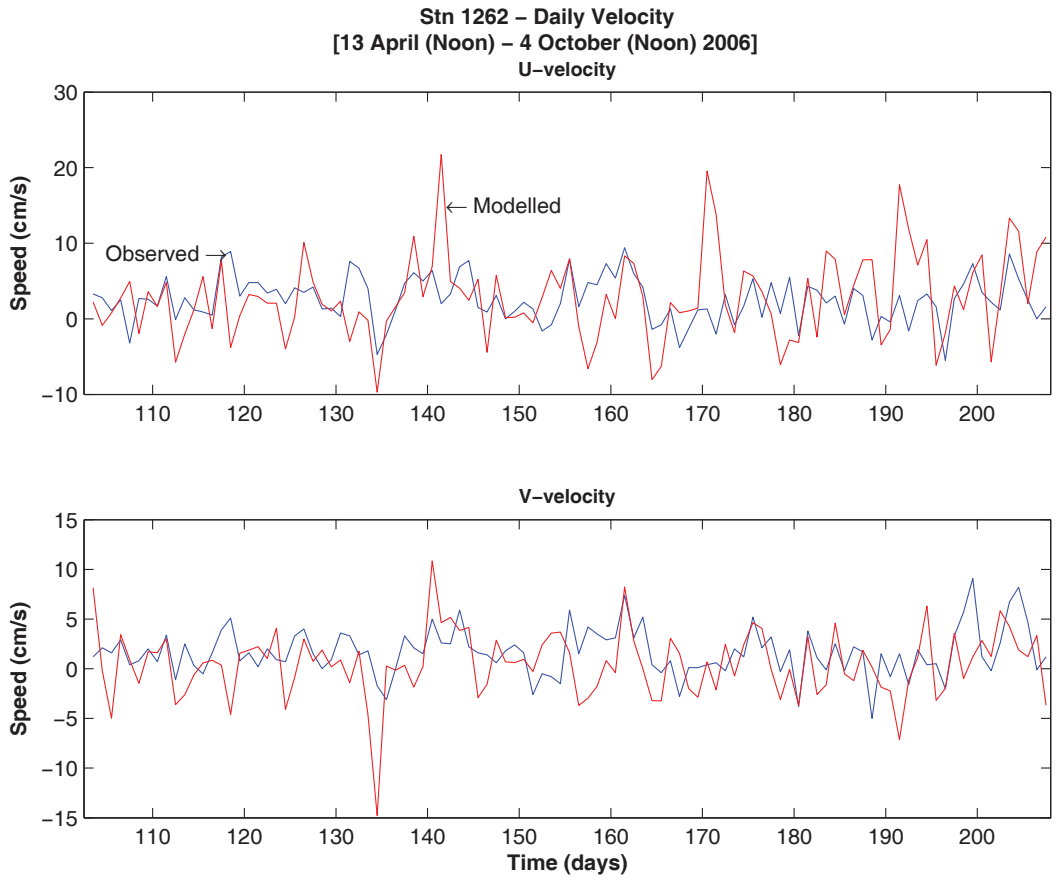

Figure 15. Daily observed and simulated East (U - component) and North (V-component) Velocity comparison at Stn 1262. Observed data were collected by Environment Canada using a two-axis MAV ultrasonic current meter with a 60min sampling frequency at 11m depth.

7. IPZ delineation from model simulated currents

IPZ-2 and IPZ-3, delineations were constructed at each intake using two-hour reverse progressive vector diagrams calculated from the modelled surface currents at the eight locations during the 24 hour storm events. Reverse progressive vector diagrams are analogous in principle to reverse particle tracking, whereby fluid parcels are continuously released at the intake are tracked backward in time such that their position within the flow domain two hours prior to release may be determined. The reverse vector progressive diagram for Kingston Central intake (figure 16) shows the effect of seasonal variability in wind direction and storm intensity on transport of fluid parcels near the intake. It can be seen that the storm event during fall is much weaker than during spring and summer with a change in direction.

The IPZ-2 and IPZ-3 were delineated as the maximum extent of the two-hour reverse progressive vector diagrams surrounding each intake. Figures 17-22 show the resulting IPZs superimposed over maps showing the intake locations. The geo-spatial coordinates of the IPZs are given in Appendix I. The nature of each IPZ is discussed below.

North Channel: The sheltering effect of Amherst Island causes the IPZs in the North Channel to be polarized by flow from the east. Due to the presence of topography the flow is weaker and oriented north-east at ALDafoe (figure 17), Fairfield (figure 19), Sandhurst (figure 17) and Bath (figure 18).

Kingston: Offshore Kingston, the IPZs (figures 21) are oriented parallel to the shore. The primary flow is from the south-west along the St. Lawrence River hydraulic axis, which is coincident with the predominant wind direction. Reversal of St. Lawrence flow during easterly storm events causes the IPZ-2 and IPZ-3 to exceed the IPZ-1 in the north-easterly direction (by 5-6km). The IPZs at both these locations overlap each other and include the majority of the Kingston waterfront with the exception of Cataraqui Bay.

St. Lawrence River: In the upper St. Lawrence River, Gananoque (figure 20) and Brockville (figure 22), the IPZs show a strong polarization from the hydraulic riverine flow. At Gananoque the effect of flow reversal during easterly wind events is reduced, relative to offshore Kingston, due to wind sheltering and reduced fetch lengths.

At the request of the CRCA, IPZ-2 and IPZ-3 delineations were also constructed using simulated depth-averaged currents. These results are presented in Appendix–II.

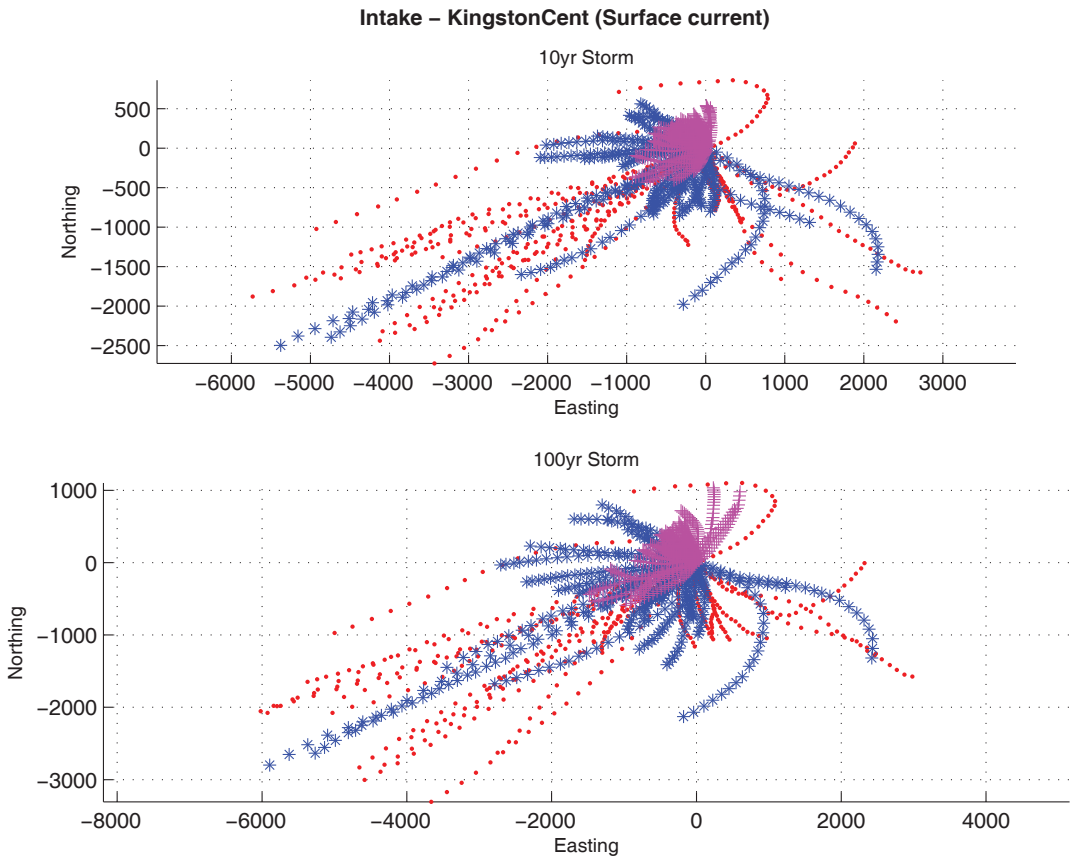

Figure 16. Reverse progressive vector diagram at Kingston Central intake location for spring (red), summer (blue) and fall (magenta) seasons (as described in section 4.1) from modeled surface currents.

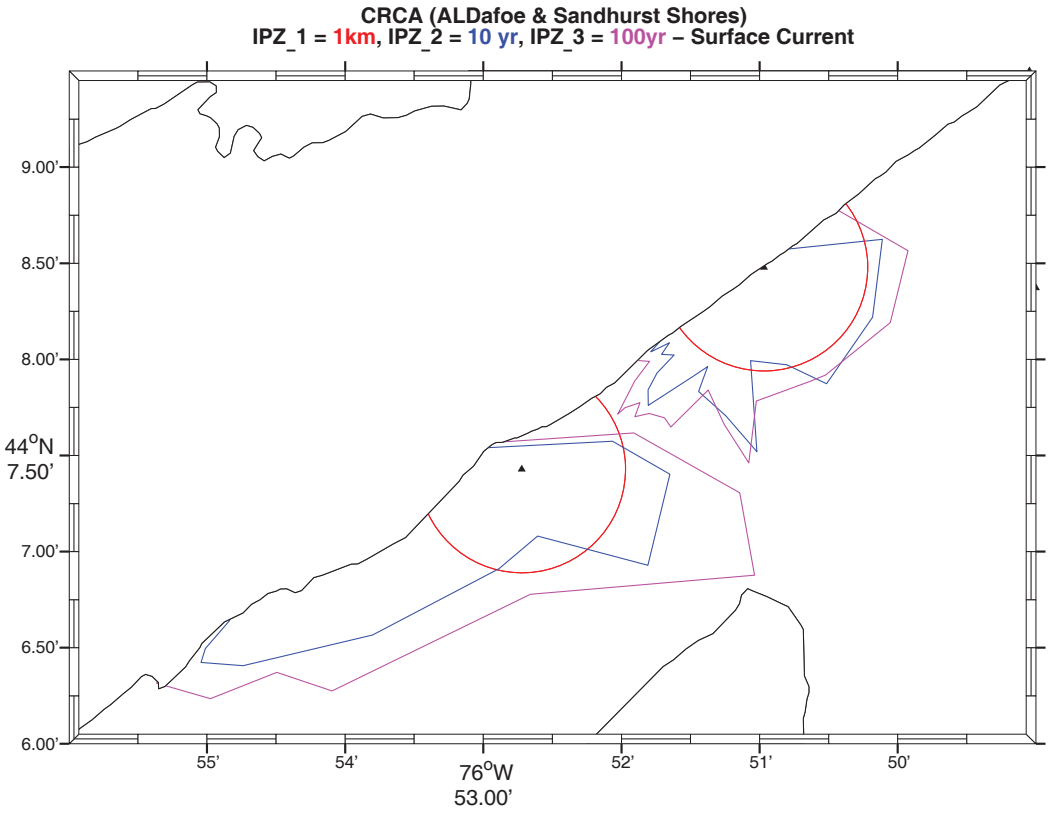

Figure 17. IPZ-1, IPZ2 and IPZ-3 calculated from modeled surface currents at A.L.Dafoe and Sandhurst Shores intake locations respectively.

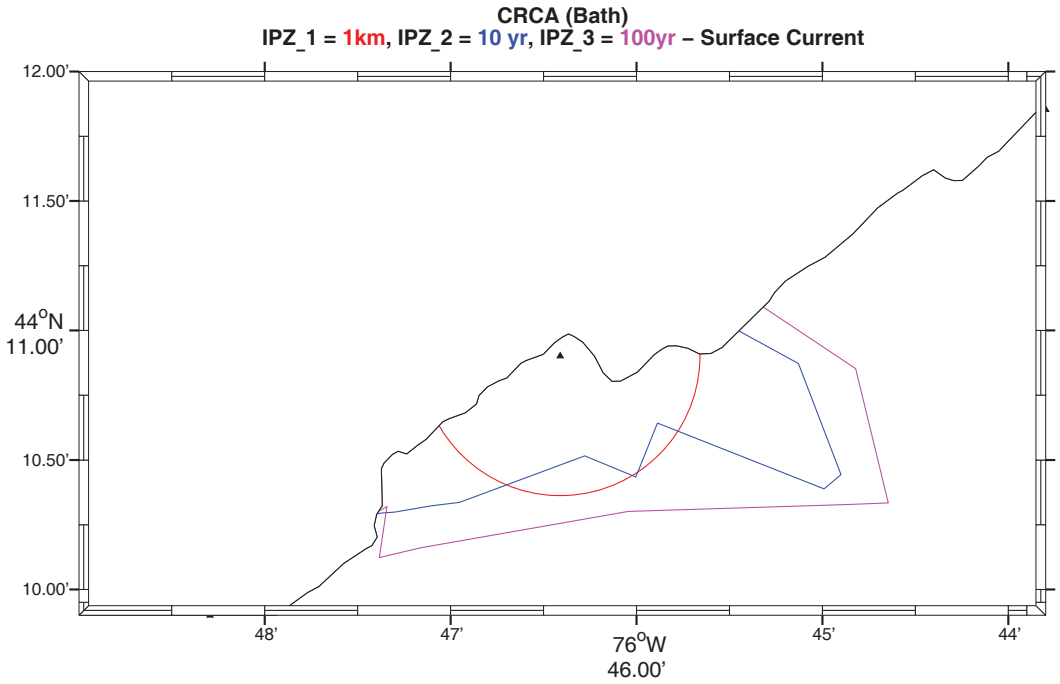

Figure 18. IPZ-1, IPZ2 and IPZ-3 calculated from modeled surface currents at Bath intake location.

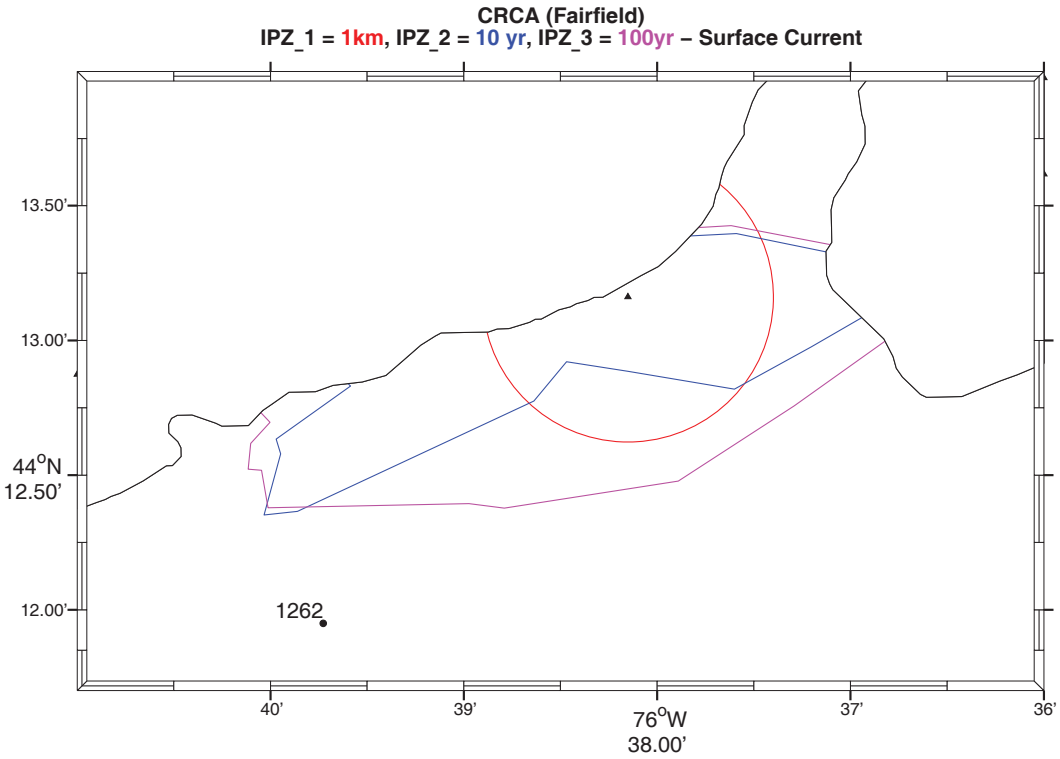

Figure 19. IPZ-1, IPZ2 and IPZ-3 calculated from modeled surface currents at Fairfield intake location.

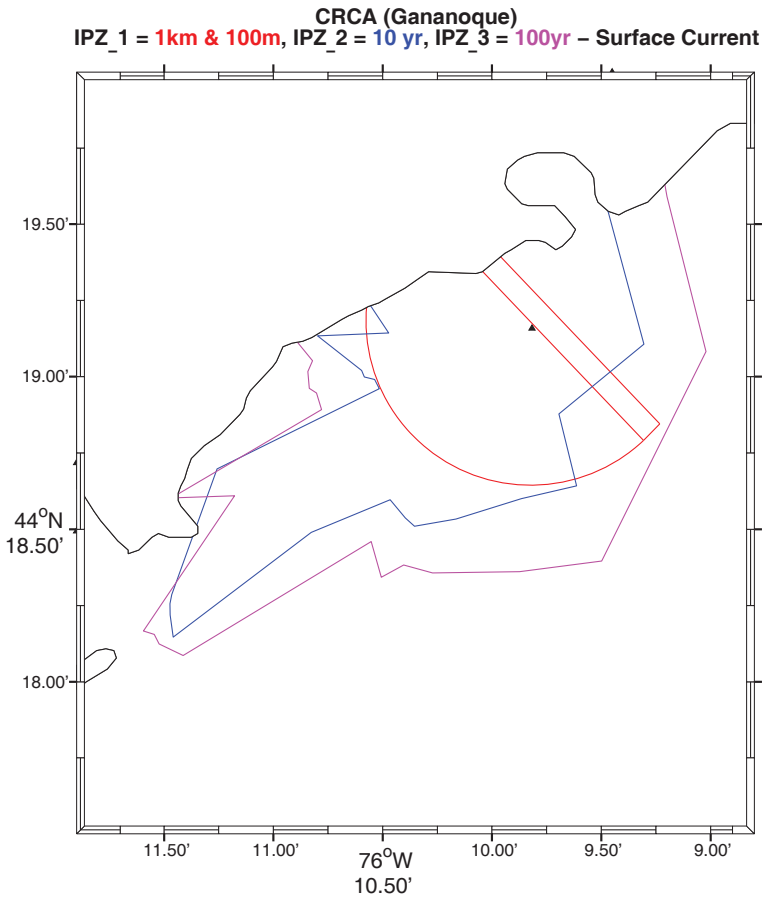

Figure 20. IPZ-1, IPZ2 and IPZ-3 calculated from modeled surface currents at Gananoque intake location.

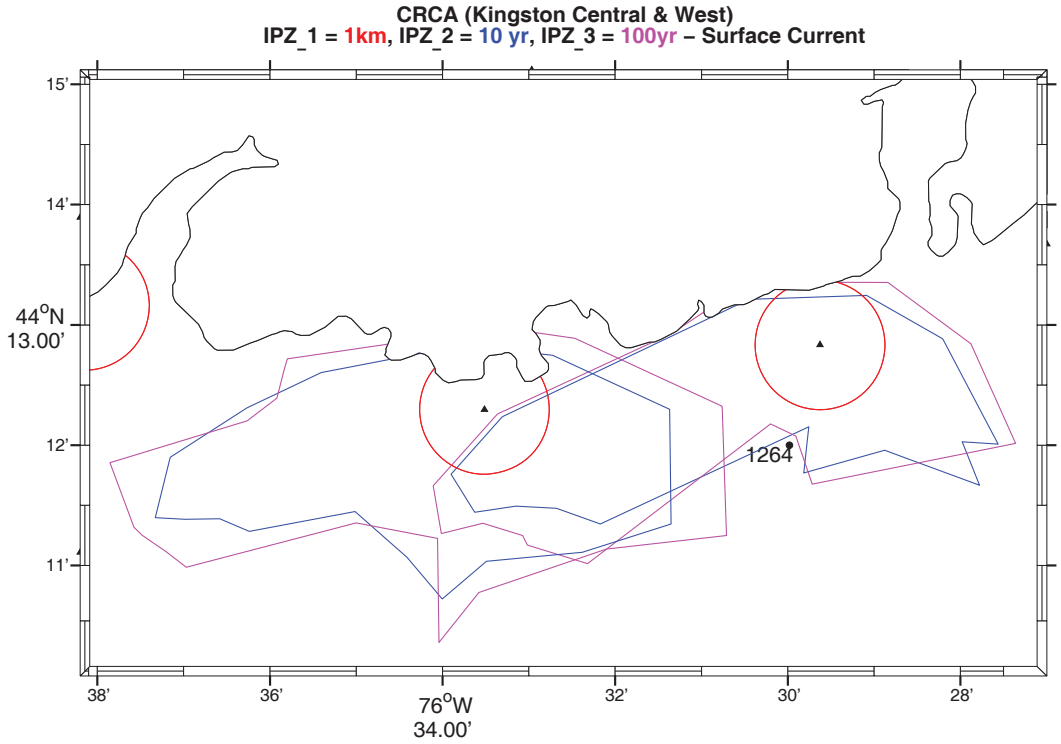

Figure 21. IPZ-1, IPZ2 and IPZ-3 calculated from modeled surface currents at Kingston Central and West intake locations.

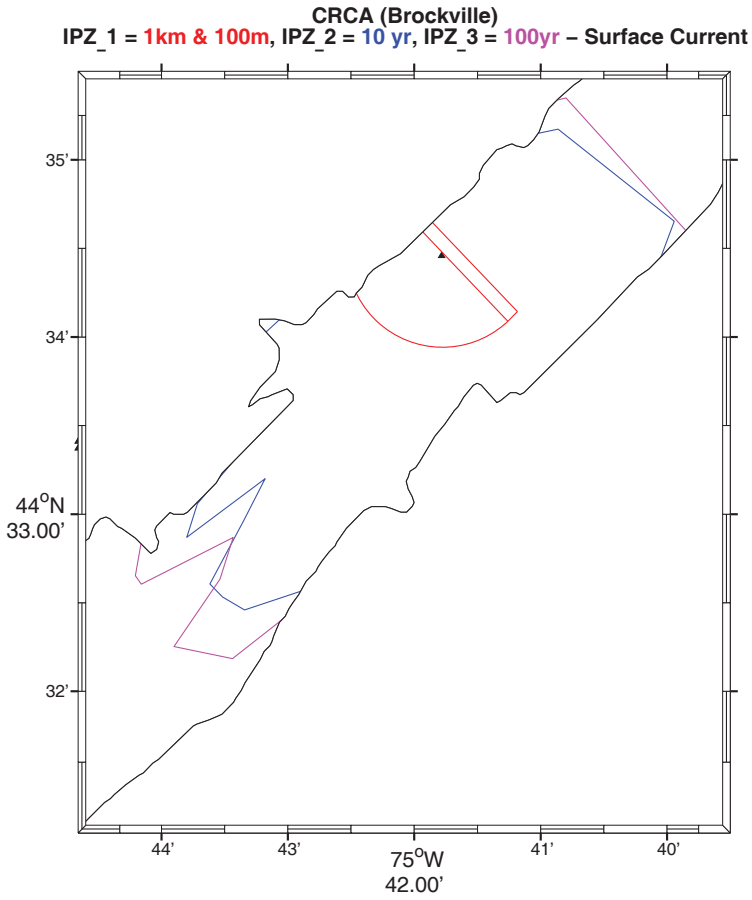

Figure 22. IPZ-1, IPZ2 and IPZ-3 calculated from modeled surface currents at Brockville intake location.

8. IPZ delineation verification against field data

To verify the IPZs from the model data, the reverse progressive vector diagrams were also calculated from the observed currents at stations 1264 (average over 1m to 2m) and 1262 (11 m depth). The observed reverse vector progressive diagrams are smaller than the modeled currents IPZs due to the inability to adjust the observed currents for 10-yr and 100-yr storm conditions. However, the shape of the vector diagrams and consequently the flow directions are consistent with the IPZs described above. This provides a measure of confidence in the model results.

Stn 1262 is located in close proximity to the Fairfield intake (figure 19). The two-hour reverse progressive vector diagram at Stn 1262 (figure 23) is smaller than the IPZs at Fairfield (figure 19) and oriented in a north-south as opposed to east -west direction. The differences in scale are discussed above and the differences in orientation are likely related to the polarizing effect of the shoreline, which is in close proximity to the intake. Stn 1264 is located in close proximity to the Kingston Central intake (figure 21). The reverse progressive vector diagram at this station (figure 25) has the same east-west orientation as the IPZ-2 (figures 16 and 21), but again is smaller in scale than the IPZs.

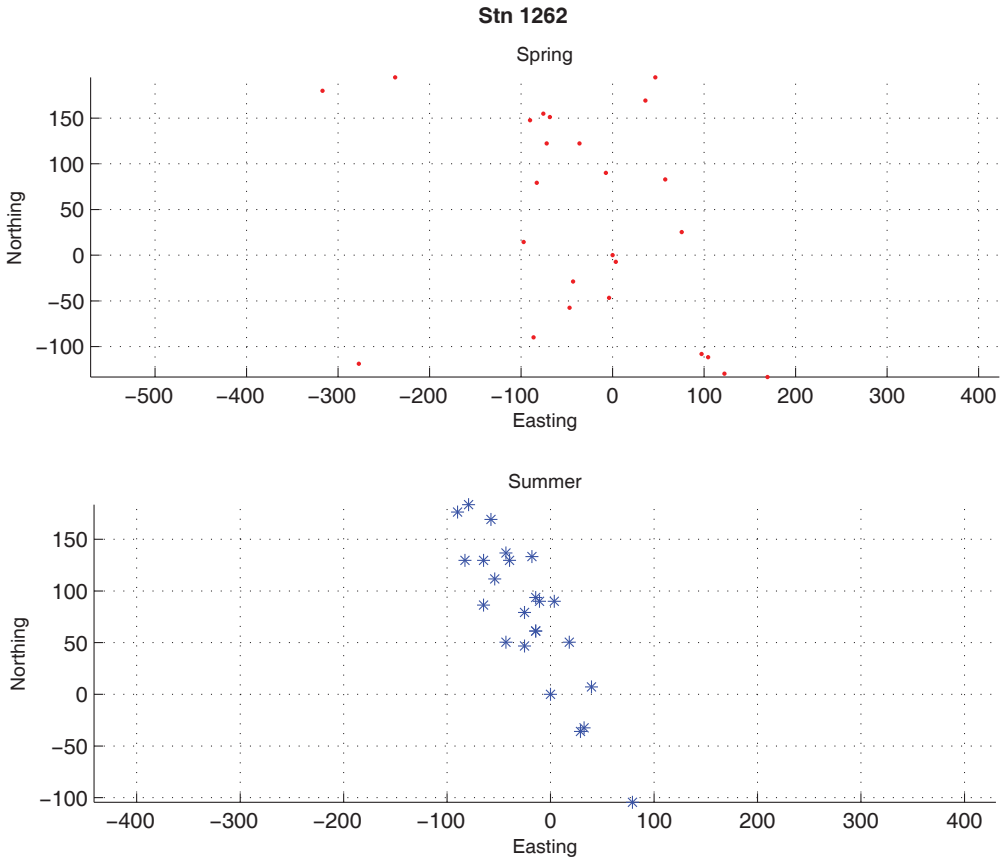

Figure 23. Reverse progressive vectors at Stn 1262 for spring (red) and summer (blue) seasons (as described in section 4.1) from observed currents.

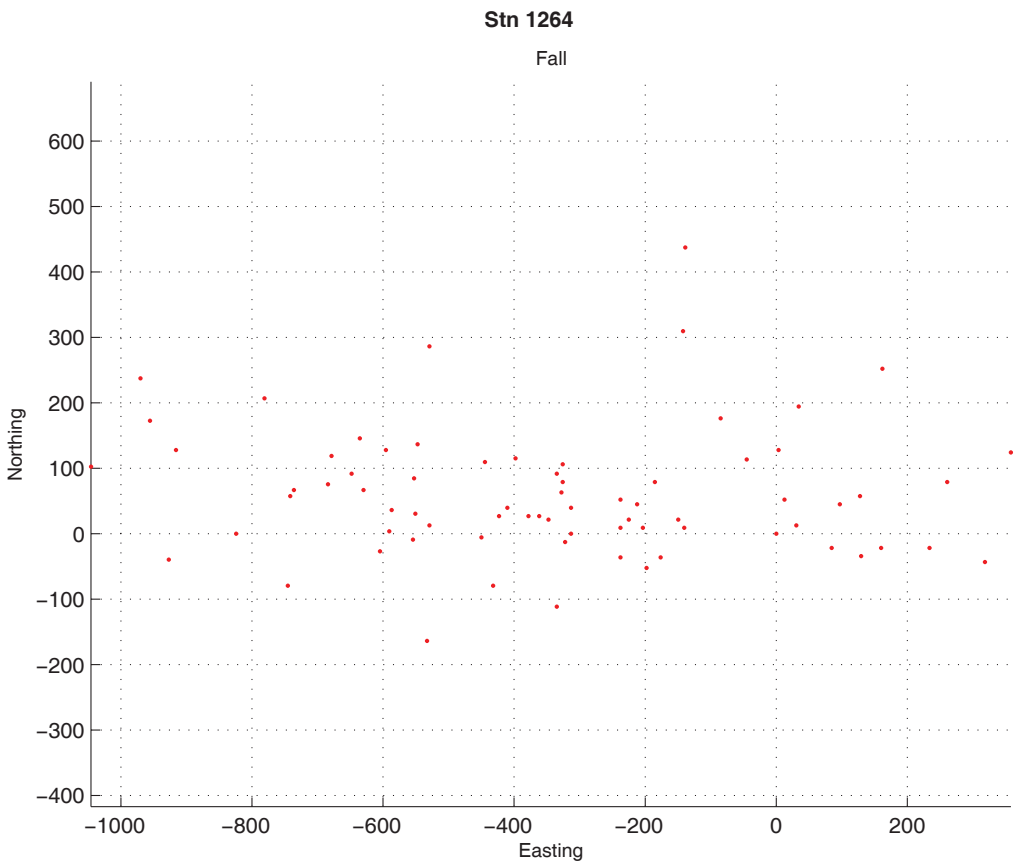

Figure 24. Reverse progressive vectors at Stn 1264 for fall (red) season (as described in section 4.1) from observed currents.

9. Conclusions

The IPZ-2 and IPZ-3 have been delineated for the eight intakes in the CRCA jurisdiction using a computational model that is validated against field data. The modeled flow structure agrees well quantitatively and qualitatively with field observations. The error in temperature is approx $2^{o}C$ through the epilimnion when the thermocline deepens during summer. The current speed errors are ~5-10 cms^{-1} and appear, at times, to be a result of inconsistencies in flow direction as opposed to momentum transfer from the wind. Current velocity errors are mostly found at exposed regions with large fetch lengths, Stns 1263 and 1264, during strong wind events and consequently may be due to the inability of the open boundary to capture momentum transfer from the 400 km fetch to the south-west. ELCOM thus reasonably captures the dynamics of the flow regimes in the near-shore region. The flow is predominantly wind-induced in the southern lacustrine portion of the domain and hydraulically-driven in the northern riverine portion.

The currents resulting from modelled storm events show seasonal variability in both magnitude and direction. The IPZ-2 and IPZ-3 generated from these currents are typically greater than the IPZ-1 and exhibit connectivity with the shoreline. The presence of the shoreline tends to polarize the flow and consequently the IPZs such that they are oriented with a longitudinal axis parallel to the shore. These IPZs are expected to provide reasonable estimates of the flow pathways to assist the CRCA in decision making and policy formulation relating to source water protection.

10. References

Hall, E. 2008. Hydrodynamic modelling of Lake Ontario. M.Sc. Thesis. Department of Civil Engineering. Queen's University.

Hodges, B. R., 2000. Numerical techniques in CWR-ELCOM, *Tech. Rep. WP 1422-BH*, Cent. for Water Res., Univ. of West Aust., Nedlands, West. Aust., Australia.

Hodges, B. R., Imberger, J., Saggio, A., and Winters, K., 2000. Modelling basin-scale internal waves in a stratified lake, *Limnol. Oceanogr*., 45, 1603-1620.

Laval, B, and Imberger, J. 2003. Modelling circulation in lakes: Spatial and temporal variations. *Limnol. Oceanogr*., 48(3), 2003, 983–994.

Laval, B, Hodges, B.R., and Imberger, J. 2003. Numerical Diffusion in 3D, Hydrostatic, Z-Level, Lake Models. *ASCE Journal of Hydraulic Engineering*: 129(3): 215-224.

National Building Code of Canada (2005). National Research Council.

Ontario Ministry of the Environment. 2005a. Assessment Report: Guidance Modules. Source Water Implementation Group.

Ontario Ministry of the Environment. 2005b. Personal Communication.

Rao, Y.R., Marvin, C.H., and Zhao, J. 2009. Application of a numerical model for circulation, temperature and pollutant distribution in Hamilton Harbour. *J. Great Lakes Res.* 35: 61-73.

Schertzer, W. M., 1987. Heat balance and heat storage estimates for Lake Erie, *J. Great Lakes Res*., 13(4):454-467.

Tsanis, I. K., Masse, A., Murthy, C.R., and Miners, K. 1991. Summer circulation in the Kingston Basin, Lake Ontario. *J. Great Lakes Res.* 17(1): 57-73.